# Optimized interferometric setup for chiral and achiral ultrafast IR spectroscopy

Dutta, Biplab ; Helbing, Jan

Abstract: We report an actively stabilized interferometer-based set-up for the detection of vibrational circular dichroism (VCD) and optical rotatory dispersion (VORD) with femtosecond laser pulses. Our approach combines and improves elements of several previous measurement strategies, including signal amplification in a crossed polarizer configuration, precise control and modulation of polarization, phase stability, tight focusing, broad-band detection and spectral interferometry. Their importance for static and transient measurements is motivated by a signal analysis based on Jones matrices and response theory. Only depending on the pump-beam polarization, the set-up can selectively detect transient VCD and VORD or transient linear birefringence (LB) and linear dichroism (LD), which usually constitute the dominant artifacts in the chiral measurements. For illustration we present transient LB and LD data of an achiral Rhenium carbonyl complex, detected simultaneously by spectral interferometry, and we analyze residual background signals in the experimental configuration for transient chiral spectroscopy.

DOI: https://doi.org/10.1364/oe.23.016449

# Optimized interferometric setup for chiral and achiral ultrafast IR spectroscopy

**Biplab Dutta and Jan Helbing***

*Department of Chemistry, University of Zurich, Winterthurerstrasse 190, CH-8057 Zurich, Switzerland*

*jan.helbing@chem.uzh.ch

**Abstract:** We report an actively stabilized interferometer-based set-up for the detection of vibrational circular dichroism (VCD) and optical rotatory dispersion (VORD) with femtosecond laser pulses. Our approach combines and improves elements of several previous measurement strategies, including signal amplification in a crossed polarizer configuration, precise control and modulation of polarization, phase stability, tight focusing, broad-band detection and spectral interferometry. Their importance for static and transient measurements is motivated by a signal analysis based on Jones matrices and response theory. Only depending on the pump-beam polarization, the set-up can selectively detect transient VCD and VORD or transient linear birefringence (LB) and linear dichroism (LD), which usually constitute the dominant artifacts in the chiral measurements. For illustration we present transient LB and LD data of an achiral Rhenium carbonyl complex, detected simultaneously by spectral interferometry, and we analyze residual background signals in the experimental configuration for transient chiral spectroscopy.



**OCIS codes:** (300.6340) Spectroscopy, infrared; (320.7100) Ultrafast measurements; (120.2130) Ellipsometry and polarimetry.

## References and links

1. L. A. Nafie, *Vibrational Optical Activity - Principles and Applications* (John Wiley & Sons, 2011).
2. B. Wang and T. A. Keiderling, "Observations on the measurement of vibrational circular dichroism with rapid-scan and step-scan FT-IR techniques," Appl. Spectros. **49**, 1347–1355 (1995).
3. F. Long, T. B. Freedman, R. Hapanowicz, and L. A. Nafie, "Comparison of step-scan and rapid-scan approaches to the measurement of mid-infrared Fourier transform vibrational circular dichroism," Appl. Spect. **51**, 504–507 (1997).
4. P. L. Polavarapu, Z. Deng, and G.-C. Chen, "Polarization-division interferometry: Time-resolved infrared vibrational dichroism spectroscopy," Appl. Spect. **49**, 229–236 (1995).
5. N. Ragunathan, N. s. Lee, T. B. Freedman, L. A. Nafie, C. Tripp, and H. Buijs, "Measurement of vibrational circular dichroism using a polarizing michelson interferometer," Appl. Spect. **44**, 5–7 (1990).
6. S. Ludeke, M. Pfeifer, and P. Fischer, "Quantum-cascade laser-based vibrational circular dichroism," J. Am. Chem. Soc. **133**, 5704 (2011).
7. A. Rüther, M. Pfeifer, V. A. Lrenz-Fonfra, and S. Lüdeke, "Reaction monitoring using mid-infrared laser-based vibrational circular dichroism," Chirality **26**, 490–496 (2014).
8. C. Guo, R. D. Shah, J. Mills, R. K. Dukor, X. Cao, T. B. Freedman, and L. A. Nafie, "Fourier transform near-infrared vibrational circular dichroism used for on-line monitoring the epimerization of 2,2-dimethyl-1,3-dioxolane-4-methanol: A pseudo racemization reaction," Chirality **18**, 775–782 (2006).
9. M. Bonmarin and J. Helbing, "A picosecond time-resolved vibrational circular dichroism spectrometer," Opt. Lett. **33**, 2086–2089 (2008).

#236664 Received 20 Mar 2015; revised 27 May 2015; accepted 27 May 2015; published 12 Jun 2015

10. M. Bonmarin and J. Helbing, "Polarization control of ultrashort mid-IR laser pulses for transient vibrational circular dichroism measurements," Chirality **21**, E298–E306 (2009).
11. J. Helbing and M. Bonmarin, "Time-resolved chiral vibrational spectroscopy," Chimia **63**, 128–133 (2009).
12. H. Rhee, J.-H. Ha, S.-J. Jeon, and M. Cho, "Femtosecond spectral interferometry of optical activity: Theory," J. Chem. Phys. **129**, 094507 (2008).
13. H. Rhee, Y.-G. June, J.-S. Lee, K.-K. Lee, J.-H. Ha, Z. H. Kim, S.-J. Jeon, and M. Cho, "Femtosecond characterization of vibrational optical activity of chiral molecules," Nature **458**, 310 (2009).
14. H. Rhee, Y.-G. June, Z. H. Kim, S.-J. Jeon, and M. Cho, "Phase sensitive detection of vibrational optical activity free-induction-decay: vibrational CD and ORD," J. Opt. Soc. Am. B **26**, 1008 (2009).
15. H. Rhee, J.-H. Choi, and M. Cho, "Infrared optical activity: Electric field approaches in time domain," Acc. Chem. Res. **43**, 1527–1536 (2010).
16. J. Helbing and M. Bonmarin, "Vibrational circular dichroism signal enhancement using self-heterodyning with elliptically polarized laser pulses," J. Chem. Phys. **131**, 174507 (2009).
17. J. Helbing and M. Bonmarin, "Vibrational chiral spectroscopy with femtosecond laser pulses," EPJ Web of Conferences **5**, 03004 (2010).
18. D. B. Shapiro, R. A. Goldbeck, D. P. Che, R. M. Esquerra, S. J. Paquette, and D. S. Kliger, "Nanosecond optical-rotatory dispersion spectroscopy - application to photolyzed hemoglobin-CO kinetics," Biophys. J. **68**, 326–334 (1995).
19. C. Niezborala and F. Hache, "Measuring the dynamics of circular dichroism in a pump-probe experiment with a babinet-soleil compensator," J. Opt. Soc. Am. B **23**, 2418–2424 (2006).
20. L. Mangot, G. Taupier, M. Romeo, A. Boeglin, O. Cregut, and K. D. Dorkenoo, "Broadband transient dichroism spectroscopy in chiral molecules," Opt. Lett. **35**, 381–383 (2010).
21. L. Lepetit, G. Cheriaux, and M. Joffre, "Linear techniques of phase measurement by femtosecond spectral interferometry for applications in spectroscopy," J. Opt. Soc. Am. B **12**, 2467–2474 (1995).
22. H. S. Chung, M. Khalil, A. W. Smith, and A. Tokmakoff, "Transient two-dimensional IR spectrometer for probing nanosecond temperature-jump kinetics," Rev. Sci. Inst. **78**, 063101 (2007).
23. D. J. Dummer, S. G. Kaplan, L. M. Hanssen, A. S. Pine, and Y. Zong, "High-quality Brewster's angle polarizer for broadband infrared application," Appl. Opt. **37**, 1194 (1998).
24. J. Helbing and P. Hamm, "Compact implementation of Fourier transform two-dimensional IR spectroscopy without phase ambiguity," J. Opt. Soc. Am. B **28**, 171 (2011).
25. J. Rehault, V. Zanirato, M. Olivucci, and J. Helbing, "Linear dichroism amplification: Adapting a long-known technique for ultrasensitive femtosecond IR spectroscopy," J. Chem. Phys. **134**, 124516 (2011).
26. X. Xie and J. D. Simon, "Picosecond circular dichroism spectroscopy: a Jones matrix analysis," J. Opt. Soc. Am. B **7**, 1673–1684 (1990).
27. S. C. Bjorling, R. A. Goldbeck, S. J. Milder, C. E. Randall, J. W. Lewis, and D. S. Kliger, "Analysis of optical artifacts in ellipsometric measurements of time-resolved circular dichroism," J. Phys. Chem. **95**, 4685–4694 (1991).
28. D. Abramavicius and S. Mukamel, "Coherent third-order spectroscopic probes of molecular chirality," J. Chem. Phys. **122** 134305 (2005).
29. J. B. Asbury, Y. Wang, and T. Lian, "Time-dependent vibration stokes shift during solvation: Experiment and theory," Bull. Chem. Soc. Jpn. **75**, 973–983 (2002).
30. J. Bredenbeck, J. Helbing, and P. Hamm, "Labeling vibrations by light: Ultrafast transient infrared spectroscopy tracks vibrational modes during photoinduced charge transfer," J. Am. Chem. Soc. **126**, 990–991 (2004).
31. B. Probst, M. Guttentag, A. Rodenberg, P. Hamm, and R. Alberto, "Photocatalytic $H_2$ production from water with rhenium and cobalt complexes," Inorg. Chem. **50**, 3404–3412 (2011).
32. D. Che, D. B. Shapiro, R. M. Esquerra, and D. S. Kliger, "Ultrasensitive time-resolved linear dichroism spectral measurements using near-crossed linear polarizers," Chem. Phys. Lett. **224**, 145–154 (1994).
33. J. Rehault and J. Helbing, "Angle determination and scattering suppression in polarization-enhanced two-dimensional infrared spectroscopy in the pump-probe geometry," Opt. Express **20**, 21665–21677 (2012).
34. J. Bredenbeck, J. Helbing, and P. Hamm, "Transient 2D-IR spectroscopy exploring the polarization dependence," J. Chem. Phys. **121**, 5943–5957 (2004).
35. A. A. Siegman, *LASERS* (University Science Books, 1986).
36. E. Polnau and H. Lochbihler, "Origin of modulated interference effects in photoelastic modulators," Opt. Eng. **35**, 3331 (1996).

## 1. Introduction

Vibrational Circular Dichroism (VCD) spectroscopy in combination with DFT calculations is an important analytic tool for determining the configuration of chiral organic molecules; VCD is also commonly used to probe the secondary structure of peptides and proteins and to detect their aggregation. VCD spectroscopy measures the differential absorption ($\Delta A_{VCD} = A_L - A_R$) of left

#236664 Received 20 Mar 2015; revised 27 May 2015; accepted 27 May 2015; published 12 Jun 2015

circular and right circular polarised infrared light, which is opposite for the two enantiomers of a chiral molecule, whose VCD spectra are therefore mirror images. The most widespread approach [1] to detecting VCD is an extension of FTIR spectroscopy where a photo elastic modulator (PEM), placed between the interferometer and the sample, modulates the light-polarization continuously from left to right circular. The differential interferogram (L minus R) is isolated by lock-in-amplification referenced to the PEM modulation frequency and Fourier transformation yields the VCD spectrum. However, the inherent poor temporal resolution of conventional FTIR spectrometers makes it impossible to resolve fast dynamics. VCD spectra have been recorded in step-scan mode [2, 3], where the time resolution would be ultimately limited by the PEM modulation frequency (30-50 kHz), but we are not aware of any transient measurements carried out in this way. In order to overcome the limitations imposed by polarization modulation, Polavarapu and coworkers used a polarization division interferometer and demonstrated time-resolved linear dichroism with microsecond time-resolution [4]. Such an interferometer can also measure VCD with very good signal to noise (S/N) [5]. Because of the low brilliance (light intensity per unit bandwidth and time) of thermal IR sources, however, S/N quickly deteriorates when integration time windows are reduced, making VCD measurements with high time resolution very difficult. Fischer and co-workers [6] have demonstrated that a tunable quantum cascade laser (QCL) can serve as an alternative, much more intense light source for steady state VCD detection. QCL-based monitoring of VCD changes in time has also been reported [7], but these experiments have not yet achieved a time resolution beyond what is already possible with commercial FTIR apparatus [8].

Some of the fundamental limitations encountered with continuous light sources can be overcome when ultrashort mid-IR laser pulses are used instead. Femtosecond IR laser pulses combine a very high peak power with a useful spectral bandwidth of 150-200 $cm^{-1}$, and the time-resolution of pump-probe experiments is no longer limited by the light intensity or the detector speed, but only by the duration of the laser pulses. In a first proof-of-principle experiment, our group dispersed femtosecond IR laser pulses in a monochromator and modulated the polarization of the narrow bandwidth output from left to right-handed circular on a shot-to-shot basis with a PEM [9]. In order to minimize artifacts [10], the light was focused through the PEM onto the sample and imaged directly onto a single element MCT detector. Static VCD spectra could be recorded with good signal to noise and, in a pump-probe experiment, changes of the chiral mid-IR signal could be detected for the first time with picosecond resolution [9, 11].

Cho and co-workers showed that it is also possible to record static VCD spectra by dispersing femtosecond laser pulses *after* they have interacted with the sample [12–15]. In order to avoid artifacts, very high quality linear polarizers were needed, which project out only one polarization component immediately behind the sample, while blocking almost completely the incident light (crossed polarizer set-up). The group used spectral interferometry, employing a replica of the laser beam, to determine simultaneously absorptive VCD and dispersive VORD (vibrational optical rotatory dispersion) spectra. An important advantage of this approach is the possibility to use an array detector to record spectra in a 'single shot' without scanning gratings or time-delays; another benefit is an intrinsic signal to noise enhancement afforded by the crossed-polarizer geometry in combination with the high light intensities [16]. Both advantages can equally be exploited in equivalent single beam measurements using elliptical polarized pulses [16, 17].

Despite many efforts, however, the crossed polarizer approach and array detection have not yet been extended to the recording of *transient* chiral signals in the infrared, although similar experiments have been carried out successfully in the UV-visible spectral range [18–20]. In this paper we address a number of experimental difficulties that have, by our experience, so far prevented a straightforward combination of our early single wavelength proof-of-principle

#236664 Received 20 Mar 2015; revised 27 May 2015; accepted 27 May 2015; published 12 Jun 2015

time-resolved experiment with signal enhancement and broad band detection techniques. Our most recent experimental set-up, which we present here in detail, is designed to overcome these problems.

## 2. Motivation

Figures 1(a) and 1(b) schematically show the two types of set-up which have previously been used for VCD measurements with femtosecond laser pulses, while Fig. 1(c) illustrates our new approach presented in this paper. The purpose of this section is to motivate our modifications, based on a brief summary of the theoretical background, which has been presented previously [13, 16]. A detailed description of the new layout follows in the next section.

### *2.1. Measurement principle*

An isotropic sample of chiral molecules with thickness $L$, absorbance $\varepsilon cL = \kappa L/\ln(10)$, refractive index $n = 1+\rho\lambda/(2\pi)$, and small optical rotation $\delta L/2 = (n_L - n_R)\pi L/\lambda$ and circular dichroism $(\varepsilon_L - \varepsilon_R)cL = \eta L/\ln(10)$ is described by the Jones matrix

$$e^{-\frac{\kappa L}{2}-i\rho L}\begin{pmatrix} 1 & \frac{\delta L}{2}-\frac{i\eta L}{4} \\ -\frac{\delta L}{2}+\frac{i\eta L}{4} & 1 \end{pmatrix} \tag{1}$$

In a crossed polarizer set-up we detect the new, perpendicular field component, created when a linear $x$-polarized light beam propagating in the $z$-direction interacts with the sample (Jones vector $\begin{pmatrix} E_0 \\ 0 \end{pmatrix}$). We call this new field component the signal field, which is given by

$$\vec{E}_S = e^{-\frac{\kappa L}{2}-i\rho L}(-\delta L/2 + i\eta L/4)E_0\vec{e}_y \tag{2}$$

$E_S$ is very small and can only be detected interferometrically, by overlap with a so-called local oscillator field

$$\vec{E}_{LO} = A(\omega)e^{i\psi(\omega,\tau)}\vec{e}_y \tag{3}$$

In conventional CD and VCD measurements, we can think of $\vec{E}_0$ and $\vec{E}_{LO} \approx \pm i\vec{E}_0$ as the two out of phase components of circular polarized light. In analogy to the differential CD measurement, in a crossed polarizer set-up we measure the change in signal when the sign of either $\vec{E}_{LO}$ or $\vec{E}_0$ (and therefore $\vec{E}_S$) is flipped:

$$\begin{aligned} S_0 &= \Delta A^+ - \Delta A^- = \log\frac{|E_{LO}+E_S|^2}{|E_{LO}-E_S|^2} \\ &\approx \frac{4}{\ln(10)}\frac{Re[E_S^* E_{LO}]}{|E_{LO}|^2} \\ &= \frac{4e^{-\kappa L/2}E_0 A(\omega)}{\ln(10)|A(\omega)|^2} Re\left[e^{i\rho L}(-\frac{\delta L}{2}+i\frac{\eta L}{4})e^{i\psi}\right] \end{aligned} \tag{4}$$

The $y$-component of perfectly circular polarized light is phase shifted by exactly $\pi/2$ with respect to the $x$-component and it experiences the same absorption and dispersion as the signal field, so

$$\begin{aligned} e^{i\psi_{circ}} &= ie^{-i\rho L} \\ A_{circ}(\omega) &= e^{-\kappa L/2}E_0 \end{aligned} \tag{5}$$

As a result, $\kappa$ and $\rho$ drop out of the expression in Eq. (4) and we obtain the CD signal $S_0 = \eta L/\ln(10)$.

#236664 Received 20 Mar 2015; revised 27 May 2015; accepted 27 May 2015; published 12 Jun 2015

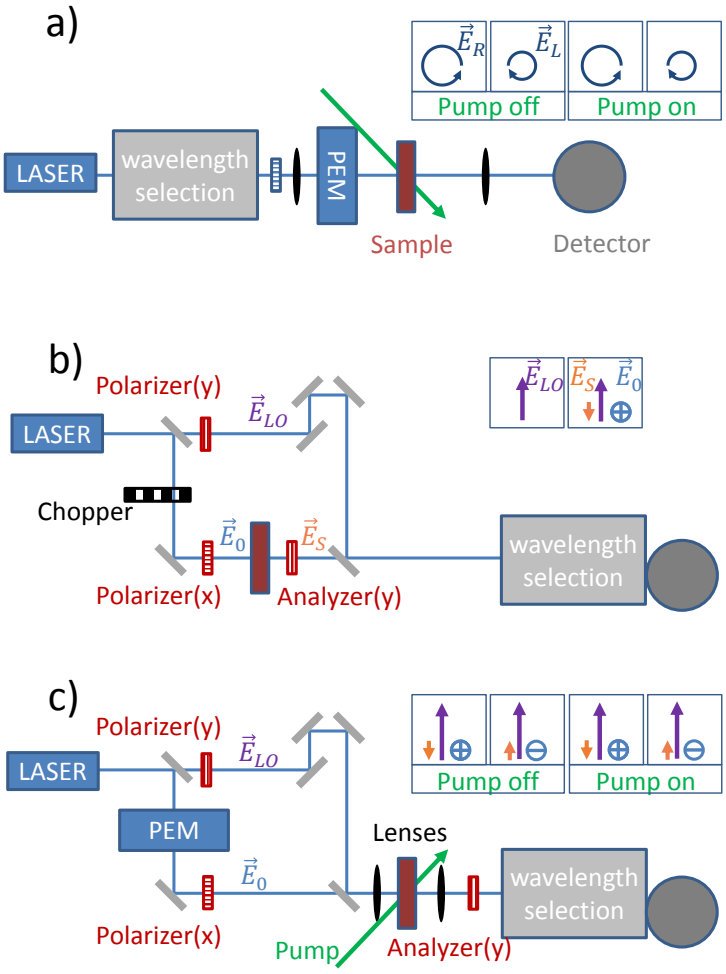


Fig. 1. Schematic comparison of laser-based VCD set-ups (a) Original scheme used for transient VCD [9]. (b) Crossed polarizer setup for spectral interferometry as introduced by Cho and coworkers [12,13] (c) New setup which combines elements of a and b. Blue circles ($\pm x$) and purple and orange arrows ($\pm y$) represent the polarization direction and sign of the different fields for four consecutive laser triggers.

In the more general case, however, the phase $\psi(\omega,\tau)$ and amplitude $A(\omega)$ of the local oscillator field is not exactly known. A second measurement must be performed under identical conditions, where the signal field $E_S$ is replaced by (a fraction of) the incident field $E_0$. In practice, this is done by tilting the analyzer by small angle $\alpha \ll 1$, which yields the second signal

$$S_\alpha = \log \frac{|E_{LO} + e^{-\frac{\kappa L}{2}+i\rho L} E_0 \alpha|^2}{|E_{LO} - e^{-\frac{\kappa L}{2}+i\rho L} E_0 \alpha|^2} \tag{6}$$

#236664 Received 20 Mar 2015; revised 27 May 2015; accepted 27 May 2015; published 12 Jun 2015

$$\approx \quad \frac{4\alpha e^{-\kappa L/2} E_0 A(\omega)}{\ln(10)|A(\omega)|^2} Re\left[e^{i\rho L} e^{i\psi}\right]$$

In a final step the full complex signals must be reconstructed from the measured real parts $S_0$ and $S_\alpha$, i.e. one needs to find the corresponding imaginary parts. This can be achieved by Hilbert or Kramers-Kronig transformation yielding

$$\begin{aligned} S_0 \quad &\rightarrow \quad \tilde{S_0} = \frac{4e^{-\kappa L/2} E_0 A(\omega)}{\ln(10)|A(\omega)|^2}(-\frac{\delta L}{2} + i\frac{\eta L}{4}) e^{i\psi} e^{i\rho L} \\ S_\alpha \quad &\rightarrow \quad \tilde{S_\alpha} = \frac{4e^{-\kappa L/2} E_0 A(\omega)}{\ln(10)|A(\omega)|^2} \alpha e^{i\psi} e^{i\rho L} \end{aligned} \tag{7}$$

In spectral interferometry, the full complex signals are usually computed by imposing causality. After inverse Fourier transform of the real signals $S_0$ and $S_\alpha$ with respect to $\omega$, all amplitude at negative times is set to zero (multiplication by the Heavyside step function $\theta(t)$) and the resultant signal is Fourier transformed back into frequency domain [21]:

$$\tilde{S_0} = F[\theta(t) F^{-1}\{S_0\}] \tag{8}$$

$$\tilde{S_\alpha} = F[\theta(t) F^{-1}\{S_\alpha\}] \tag{9}$$

The two signals can now be divided which yields the absorptive and dispersive spectra:

$$S^{\text{out of phase}} \quad = \quad Im[\tilde{S_0}/\tilde{S_\alpha}] = \frac{\eta L}{4\alpha} \tag{10}$$

$$S^{\text{in phase}} \quad = \quad Re[\tilde{S_0}/\tilde{S_\alpha}] = -\frac{\delta L}{2\alpha} \tag{11}$$

Multiplication with appropriate scaling factor then yields the circular dichroism and optical rotation spectra:

$$\Delta A_{VCD}[OD] \quad = \quad \frac{\eta L}{\ln(10)} = \frac{4\alpha[rad]}{\ln(10)} S^{\text{out of phase}} \tag{12}$$

$$VORD[rad] \quad = \quad \frac{\delta L}{2} = -\alpha[rad] S^{\text{in phase}} \tag{13}$$

Note that although both VCD and VORD spectra are obtained simultaneously, the signal processing relies on a Kramers-Kronig transformation in a restricted spectral window, just like a post-measurement determination of the VORD spectrum from a measured VCD spectrum. Based on these equations and the schematic comparison of different laser-based setups in Fig. 1, the new elements in our current approach can be discussed:

### *2.2. The crossed polarizer advantage*

The magnitude of the chiral signal $S_0$ is proportional to the ratio $|E_0|/|A(\omega)|$ or, in other words the ratio of the *x*-polarized incident field and the *y*-polarized local oscillator field. With respect to a conventional CD measurement with circular polarized light (or a polarizing interferometer without additional analyzer), where $|E_0| = |A(\omega)|$ this can afford significant signal enhancement. With typical femtosecond laser pulses, $E_0$ can be made 5-10 times larger than the local oscillator $|A(\omega)|$, which still remains strong enough to nearly saturate the MCT detector. Measurements with thermal light sources, on the other hand, are usually light-limited, meaning that any increase of $E_0$ at the cost of $A(\omega)$ would lead to increased noise levels caused by poor illumination of the detector. Most importantly, after the high-quality analyzer immediately behind the sample, polarization-sensitive optics like a monochromator grating or mirrors can no

#236664 Received 20 Mar 2015; revised 27 May 2015; accepted 27 May 2015; published 12 Jun 2015

longer distort the chiral signal by affecting differently the signal and local oscillator fields. It is therefore possible to disperse the broad band femtosecond pulses and record them with an array detector as in conventional time-resolved IR spectroscopy. Spectra can be recorded much more quickly (in principle with a single laser shot) and afford highly correlated noise, which makes it easier to identify small features.

### 2.3. Polarization modulation

Polarization modulation in conventional VCD measurements ideally corresponds to a periodic reversal of either the signal or the local oscillator field, or, in practice, to a $\lambda/(2c)$ time shift of one polarization component with respect to the other. When these two perpendicular polarized fields propagate as separate beams as in Fig. 1(b), VCD may also be measured by periodically blocking one of them with a chopper [13]. However, in that case the measured signals are only half as large as with a modulator scheme shown in Fig. 1(c). It is much more precise to induce an exact $\lambda/(2c)$ time shift with a PEM and define the polarization state afterwards with a high quality polarizer than to directly modulate the polarization state in a single beam experiment [10]. In the first case, only the intensity of consecutive pulses must be compared when optimizing the PEM retardation. At the same time the detector sees only the other, $y$-polarized, unmodulated beam, which is not affected by a possible small PEM-modulation of the beam divergence (see appendix). This is also a big advantage over some of our earlier attempts to realize crossed-polarizer schemes in single beam experiments [10, 17].

### 2.4. Phase stability

For a proper signal processing according to Eq. (8), the two signals $S_0$ and $S_\alpha$ must be measured under identical conditions, i.e. the phase $\psi(\omega,\tau)$ must not change over the course of the two measurements. For example, if the local oscillator is a time-shifted copy of the $x$-polarized beam, $\psi(\omega,\tau) = (\omega-\omega_0)\tau$ and $S_\alpha$ exhibits regular fringes in frequency, with a characteristic spacing inversely proportional to the time shift $\tau$. Consequently, $\tau$ must be stable within a small fraction of the light period during the measurements. Active beam path length stabilization is required to enable the long data averaging necessary for transient VCD measurements.

### 2.5. Co-propagation of the local oscillator beam

Both Eqs. (4) and (6) contain contributions due to absorption and dispersion, which may change in time or by laser excitation in a time-resolved experiment. However, $\kappa L$ and $\rho L$ disappear from the expressions for $S_0$ and $S_\alpha$ if the local oscillator passes through the sample, just as in the case of circular polarized light. The new scheme Fig. 1(c) combines this advantage of the single beam experiment (scheme a) with the independent intensity and polarization control of $E_S$ and $E_{LO}$. Similar considerations apply in transient 2D-IR spectroscopy, where the LO beam must also be guided through the excited sample volume [22].

### 2.6. Beam focusing

In order to reach excitation levels of at least a few percent in pump-probe experiments, the laser beams must be tightly focused to a spot size of approximately 100 $\mu$m diameter on the sample. This must be achieved without perturbing the high quality of polarization of the individual beams and thus the extinction of the crossed-polarizer set-up. Tight focusing also allows to exchange the laser-excited sample on a pulse-to-pulse basis in a flow cell.

#236664 Received 20 Mar 2015; revised 27 May 2015; accepted 27 May 2015; published 12 Jun 2015

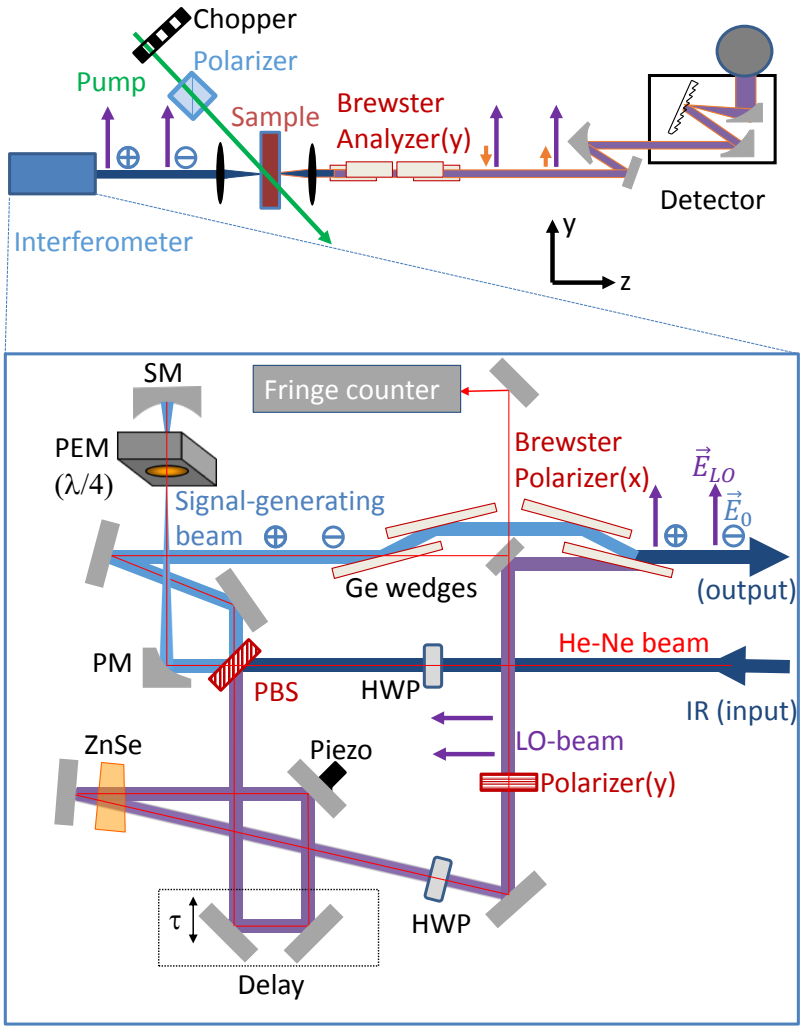


Fig. 2. Detailed view of the new setup. PBS: polarising beam splitter, Piezo: Piezo-controlled mirror, ZnSe: Zinc selenide wedge, PEM: Photo elastic modulator, PM: off axis parabolic mirror, SM: spherical mirror, HWP: Zero-order half wave-plate.

## 3. Setup

A detailed layout of our new setup is shown in Fig. 2. Infrared light from a mid-IR optical parametric amplifier (OPA) is split by a polarizing beam splitter (PBS, holographic wire grid polarizer, Thorlabs WP25H-B, extinction ratio $\approx 10^{-2}$) into two parts. The horizontally polarized component is transmitted and vertically polarized light is reflected. The relative strength of transmitted and reflected beams can be adjusted by a half-wave plate (HWP) in front of the beam splitter. The transmitted beam makes a double pass through a ZnSe (zinc selenide) photo-elastic modulator (PEM, Hinds Instruments) placed at the focal point of a telescope, which acts as a quarter-wave plate and causes a $\pm 90^\circ$ rotation of the polarization. The returning beam is thus reflected by the wire-grid beam splitter and is guided through a Brewster angle germanium

#236664 Received 20 Mar 2015; revised 27 May 2015; accepted 27 May 2015; published 12 Jun 2015

wedge polarizer (extinction ratio $< 10^{-7}$) [23], which defines the $x$-direction in the laboratory. We call this beam the signal-generating beam.

The second arm of the interferometer comprises a delay line, a ZnSe wedge, and a $MgF_2$ zero order half-wave plate (HWP, Bernhard Halle Nachf., RZM4.15L), which rotates the polarization of the initially vertically polarized beam. This beam is called local oscillator (LO) beam. The polarization of the LO-beam is cleaned by a free-standing wire grid polarizer (Infraspecs P03, extinction ratio $< 10^{-4}$) oriented in the $y$-direction, such that its intensity can be fine-tuned independently by adjusting the wave plate. In order not to destroy the purity of polarization, we use the last wedge of the Brewster angle polarizer in the signal-generating beam to unite signal-generating and LO-beams. As a result, this interferometer synthesizes pairs of pulses with very pure orthogonal polarization with freely adjustable intensity and delay. They are focused into the sample by a $CaF_2$ lens of 10 cm focal length and collimated again by an identical lens before passing the analyzer. The analyzer design is identical to that of the pump-beam polarizer and consists of four germanium wedges, placed in a solid mount at Brewster angle (14°) as shown in Fig. 2(a). It only transmits the $y$-polarized LO ($E_{LO}$) and the chiral signal ($E_S$) but completely blocks the $x$-polarized signal-generating beam ($E_0$). The transmitted light is then dispersed in a monochromator by a 300 lines/mm grating onto a nitrogen cooled MCT array detector (MercuryCadmiumTelluride, Infrared Associates, 2x32 pixels), which is read out on a shot-to-shot basis. The second array of this detector records a fraction of the OPA output which is split off before the interferometer and used as a reference to correct for intensity fluctuations. The PEM is oriented at 45° with respect to the incoming light polarization and acts as a quarter-wave plate with alternating sign. The femtosecond laser is synchronized to the PEM to ensure that every pulse precisely meets the trough or the crest of the modulation, as described in detail in reference [10]. A double pass through the PEM thus alternately turns the electric field vector of the signal-generating beam into the $\pm x$ direction (indicated by $\oplus$ and $\ominus$ in Fig. 2 ). The PEM is placed at the focal point of a telescope to minimize spatial modulation of the beam (see appendix). This and the double pass also allow us to drive the PEM with low voltage, which minimizes electronic noise. The thickness of the ZnSe wedge in the LO beam (1.5875 cm) matches that of the PEM in the pump-beam and introduces similar frequency dispersion (chirp). We observed highly unsymmetrical temporal interferograms between pump and LO beam without the ZnSe wedge in the LO beam path. A helium neon laser beam co-propagates 4 cm above the IR beams, either via the same mirrors or (in the case of the beamsplitters and the telescope) via optics on shared mounts. The He-Ne laser interference serves as a feedback signal to actively stabilize the path difference in the interferometer to within approximately 100 nm via a piezo-mounted mirror in the LO-beam path. In combination with quadrature counting, the HeNe interferogram also permits precise delay tracking and FTIR operation of the set-up, when single element MCT detectors replace the monochromator and array detector and $\tau$ is scanned rapidly [24].

## 4. Results and discussion

### *4.1. Static measurements*

In order to test the performance of our setup for static chiral measurements, we recorded spectra for nickel-sparteine complexes [Ni((-)-sparteine)]$Cl_2$ and [Ni((+)-sparteine)]$Cl_2$, dissolved in $CDCl_3$ at a concentration of 0.7 M. The samples were circulated in a 100 $\mu$m thick flow cell to mimic the conditions in a transient measurement.

The top panel of Fig. 3 shows the signals $S_0$ for the two enantiomers in blue and red, respectively, while the green line represents the solvent background. The enantiomers clearly show opposite signals, while the achiral interferograms $S_\alpha$ of the leaked signal-generating beam and the LO in the second panel are almost indistinguishable. The corresponding absorptive (VCD)

#236664 Received 20 Mar 2015; revised 27 May 2015; accepted 27 May 2015; published 12 Jun 2015

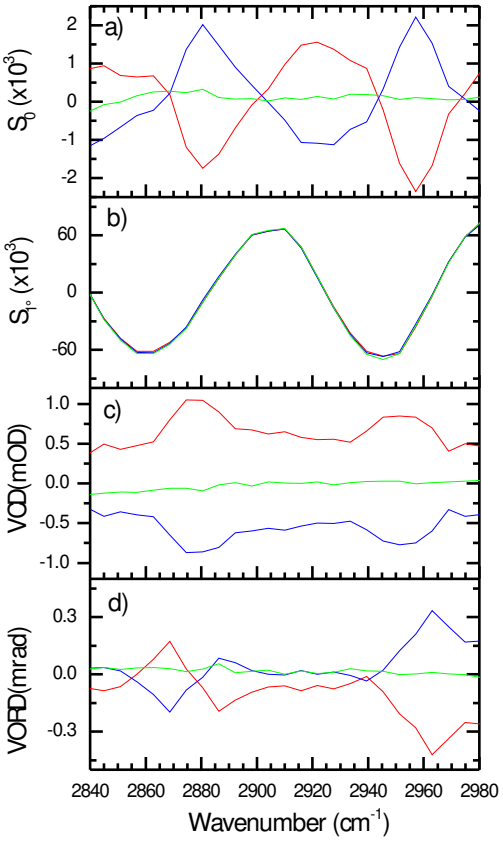


Fig. 3. Spectral interferograms $S_0$ and $S_\alpha$ recorded with crossed polarizers (a) and a slightly tilted analyzer (b), $\alpha = 1^\circ$. Amplitudes correspond to differential absorption (mOD). Red: [Ni((-)-sparteine)]$Cl_2$, blue: [Ni((+)-sparteine)]$Cl_2$, green: $CDCl_3$ solvent background. The path difference between the two arms of the interferometer was $\approx 450$ fs. Corresponding VCD (c) and VORD (d) spectra computed using Eqs. (8) and (12).

and dispersive (VORD) spectra, obtained by applying Eqs. (8) and (12) are plotted in Fig 3(c) and 3(d). When the two arms of our interferometer have almost equal length (to within one wavelength of the infrared light), the interferometer should act like a zero order wave plate and can be viewed as a very precise synthesizer of a single femtosecond laser pulse with arbitrary polarization. For example, when the path difference is $\pm\lambda/4$, it should produce elliptical pulses of opposite handedness, and $S_0$ should be directly proportional to the absorptive VCD spectrum, just like in our earlier single beam measurements [16]. Likewise, a pathlength difference modulated between 0 and $\lambda/2$ should yield linear polarized pulses for a direct measurement of the dispersive VORD spectrum. In Fig. 4 we show a series of signals $S_0$, acquired with path differences within one wavelength from zero. Comparison with Fig. 4 immediately shows that none of the spectra are either purely absorptive (VCD) or dispersive (VORD) over the whole spectral window, a direct consequence of the spectral dependence of $\psi(\omega,\tau)$ caused by different dispersion in the two interferometer arms. For comparison, also in conventional VCD measurements with FTIR spectrometers, the instrument-dependent spectral phase must be known in order to

#236664 Received 20 Mar 2015; revised 27 May 2015; accepted 27 May 2015; published 12 Jun 2015

extract the VCD spectrum from the chiral interferogram. In femtosecond experiments with a

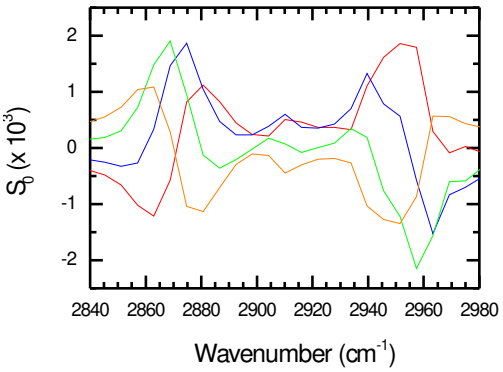


Fig. 4. $S_0$ spectra of [Ni((-)-sparteine)]$Cl_2$ near interferometer delay $\tau = 0$, raised in four steps of $\Delta\tau = 2.11$ fs, corresponding to $0.22\lambda_{IR}/c$.

spectrometer, on the other hand, the spectral phase is eliminated by division with the complex achiral signal $\tilde{S}_\alpha$ (Eq. (12)), of which we can only measure the real part $S_\alpha$ (Fig. 3(b)). For the Kramers-Kronig transform Eq. (9) we need a sufficiently large delay $\tau$ between local oscillator and the signal-generating field in order to minimize the intensity of $F^{-1}\{S_\alpha\}$ near $t = 0$ and thus avoid artifacts. The optimal interferometer delay is thus not equivalent to a zero order wave plate but rather corresponds to tens of cycles of the IR fields. We obtained fully reproducible VCD and VORD spectra in the interval 0.2 ps$< \tau <$1 ps. Beyond the upper limit for $\tau$, spectral fringes are no longer sufficiently resolved by our 32 pixel MCT array detector. Concerning the choice of the analyzer tilt angle $\alpha$ for the measurement of $S_\alpha$, one degree turned out to be sufficient for very good signal to noise affording even shorter averaging than for $S_0$. Much larger tilt angles should be avoided in order to limit the alignment and light level changes at the detector with respect to the $S_0$ measurements. Although the intensity ratio of signal-generating and LO beams does not change the amplitudes of the final VCD and VORD spectra, the individual signals $S_0$ and $S_\alpha$ are directly proportional to $|E_0|/|E_{LO}|$ in the crossed polarizer approach, and signal to noise can be significantly enhanced by increasing this ratio. When doing so, the limiting factor in IR-measurements is almost always the available light intensity (long before for this proportionality is no longer valid [25]). In our case, the poor transmission ($\approx$30%) of the Germanium wedge polarizer, and a further 40% intensity loss inside the interferometer mean that the signal-generating beam can only be 25 times more intense than the LO beam at the sample ($|E_0|/|E_{LO}| \approx 5$). Doubling this factor and thus the signal to noise ratio would require a fourfold increase in laser intensity.

### *4.2. Transient measurements*

For our pump-probe experiments we periodically block the visible pump beam at one quarter of the laser frequency and thus measure the intensity at the detector twice for each modulator state (see Fig. 1). This allows us to calculate $S_0$ (Eq. (4)) and hence $\tilde{S}_0$ (Eq. (8)) once with the pump laser on and once with the pump laser off. In addition, $\tilde{S}_\alpha$ must be determined independently from a measurement with tilted analyzer. We found that pump-induced changes of $\tilde{S}_\alpha$ are usually negligible, meaning that it needs to be measured only once and not separately for each pump-probe delay. In analogy with Eq. (10) we can thus evaluate the transient out of phase

#236664 Received 20 Mar 2015; revised 27 May 2015; accepted 27 May 2015; published 12 Jun 2015

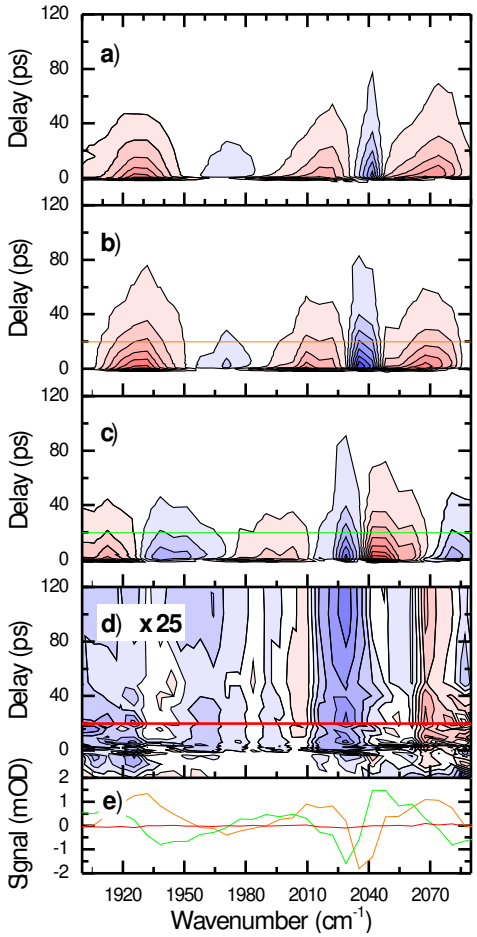


Fig. 5. Transient LD and LB signals of [Re(py)$(CO)_3$(bpy)] dissolved in acetonitrile with 400 nm excitation. (a) LD measurement with only one IR beam and the analyzer at $\pm 12^\circ$ (b) LD (in phase signal) and (c) LB (out of phase signal) obtained by spectral interferometry as described in the text ($\tau$ =150 fs, 1 contour level= 0.5 mOD). The 400 nm beam was polarized at 45° with respect to LO and signal generating field. (d) Out of phase signal with vertical pump polarization (1 contour level= 20 $\mu$OD), where only chiral signals (transient VCD) should be seen. e) Horizontal cuts along the orange, green and red lines (20 ps pump-probe delay) in b, c and d.

and in phase signals:

$$\Delta S^{\text{out of phase}} = Im[\frac{\tilde{S_0}^{\text{pump on}}}{\tilde{S_\alpha}}] - Im[\frac{\tilde{S_0}^{\text{pump off}}}{\tilde{S_\alpha}}] \quad (14)$$

$$\Delta S^{\text{in phase}} = Re[\frac{\tilde{S_0}^{\text{pump on}}}{\tilde{S_\alpha}}] - Re[\frac{\tilde{S_0}^{\text{pump off}}}{\tilde{S_\alpha}}] \quad (15)$$

In an ideal setup, where the pump beam polarization is either perfectly parallel or perpendicular to $\vec{E}_0$ and $\vec{E}_{LO}$, these signals represent, up to the appropriate scaling factors, the transient

#236664 Received 20 Mar 2015; revised 27 May 2015; accepted 27 May 2015; published 12 Jun 2015

Table 1. Dominant contributions to the in-phase and out-of phase transient signals in a crossed polarizer setup for different orientations of the pump-pulse polarization. The factor $\ln(10)/4 \approx 0.58$ for $\alpha$ in radians or $180\ln(10)/(4\pi) \approx 32.98$ for $\alpha$ in degrees is due to the different units used in absorption and rotation angle measurements.

| | $\theta$ | $\alpha$[rad]$\Delta S^{\text{out of phase}}$ | $\alpha$[rad]$\Delta S^{\text{in phase}}$ |
|---|---|---|---|
| 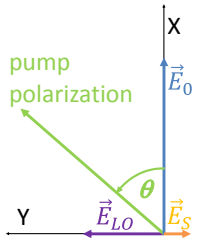  | $0°, (90°)$ | Transient VCD [OD] $\times \frac{\ln(10)}{4}$ (absorptive) | Transient VORD [rad] (dispersive) |
| | $45°$ | Transient LB [rad] (dispersive) | Transient LD [OD] $\times \frac{\ln(10)}{4}$ (absorptive) |

VCD and ORD spectra respectively. However, the potential distortion of time-resolved circular dichroism signals by pump-induced linear dichroism (LD) and linear birefringence (LB) have already been discussed in the context of the first CD experiments with visible picosecond lasers by Xie and Simon [26, 27]. In our description of the experiment on the basis of linear polarized fields and simultaneous consideration of both absorptive and dispersive contributions the very close similarity of the chiral and the achiral transient measurements (and hence the potential danger of misinterpretation) becomes even more evident.

Essentially, chiral and the achiral pump-probe experiment differ only in the polarization direction of the excitation pulse with respect to the probe fields. According to non-linear response theory, the transient signal of an isotropic solution is proportional to the orientational average $\langle WWXY \rangle$, where $Y$ is the polarization direction of the LO, which is transmitted by the analyzer, $X$ is the polarization of the signal-generating beam and $W$ is the polarization of the visible excitation beam. The signal is purely chiral if and only if $W \equiv X$ or $W \equiv Y$ (or $W \equiv Z$). If $W$ has both $X$ and $Y$ components, on the other hand, there are necessarily linear dichroism and linear birefringence contributions. They are strongest when $W = X + Y$, i.e. when the polarization of the pump pulse is rotated by an angle $\theta = 45°$ with respect to both $E_0$ and $E_{LO}$ (we neglect the small $Z$-component introduced by the different propagation directions). The orientational average determining the signal in this case is:

$$\begin{aligned} \langle (X+Y)(X+Y)XY \rangle &= \langle XXXY \rangle + \langle YYXY \rangle \\ &+ \langle XYXY \rangle + \langle YXXY \rangle \end{aligned} \tag{16}$$

The first line in this equation gives rise to the very small, electric dipole-forbidden transient chiral signal, while the second line contains the usually much larger dipole-allowed linear dichroism and linear birefringence contributions (note the identity $\langle XYXY \rangle + \langle YXXY \rangle = \langle YYYY \rangle - \langle XXYY \rangle$ ) [28]. The dominant contributions to the transient signals $\Delta S^{\text{out of phase}}$ and $\Delta S^{\text{in phase}}$ for the two limiting cases of pump-beam polarization are summarized in Table 1.

As data acquisition and processing for transient chiral and achiral signals are identical we decided to test the performance of our setup by recording pump-induced LD and LB of the achiral metal carbonyl complex [Re(py)$(CO)_3$bipy] in acetonitrile, setting the 400 nm pump pulse polarization to 45°. Excitation at this wavelength causes an ultrafast metal to ligand electron transfer, which is stabilized in a long-lived triplet state, characterized by a blue-shift of the

#236664 Received 20 Mar 2015; revised 27 May 2015; accepted 27 May 2015; published 12 Jun 2015

CO vibrations [29–31]. Anisotropy and hence linear dichroism and birefringence are induced by the preferential excitation of molecules whose electronic transition dipole moment is aligned with the pump polarization. The transient signals $\Delta S^{\text{in phase}}$ (LD) and $\Delta S^{\text{out of phase}}$ (LB) of the CO stretch vibrations are shown in Figs. 5(b) and 5(c). For comparison, Fig. 5(a) shows the transient LD signal measured in an already established way, by blocking one interferometer arm and changing the orientation of the analyzer between $\pm\beta$. For $\beta = 45^\circ$ this is the conventional LD signal $(\Delta A_\parallel - \Delta A_\perp)$, which is enhanced by a factor $\cot\beta$ for $\beta < 45^\circ$ [25,32,33]. The signal decay on a 20 ps timescale is due to rotational diffusion of the complex, which renders the sample isotropic again [29,34].

The good agreement between Figs. 5(a) and 5(b) shows that spectral interferometry can be efficiently used for highly sensitive transient measurements in a crossed-polarizer configuration. The recording and processing of transient LB and LD signals is completely analogous to that of transient VCD and VORD signals, for which the visible pump beam polarization must be set exactly to $X$. This means that possible LD and LB artifacts on top of a transient chiral signal can be identified in a complementary measurement under almost identical experimental conditions. For example, both transient VCD and LB are out of phase signals and formally correspond to a $\pi/2$ phase shift between the LO and the signal-generating beam. They may both resemble the derivative of the transient absorption signal and can thus be easily confounded.

In our achiral test sample, the transient LD and LB signals should completely vanish when the 400 nm polarization is aligned perpendicular to that of the LO. This seems to be the case in Fig. 5(d), showing $\Delta S^{\text{out of phase}}$ measured with a $X$-polarized pump beam, where we can no longer identify any signal that decays on the timescale of rotational diffusion. However, we observe a residual signal of the order of $10^{-4}$ OD, approximately 3-4% of the LB amplitude at 45° pump orientation, which lasts for more than 100 picoseconds and is thus not related to pump-induced anisotropy. We found that this residual signal had a different shape and a larger amplitude when the interferometer delay was changed from 150 fs to 500 fs. This could point to an artifact due to a pump-induced phase change between LO and the signal-generating beam, which we have tried to minimize in our set-up by co-propagating both through the same spot on the sample. In order to test this hypothesis, we have repeated the complete pump-probe scan with a tilted analyzer, recording separate $\tilde{S}_\alpha$ for each pump-probe delay and chopper state. However, we found no difference between using these individual reference signals, which should be sensitive to pump-induced phase shifts, or a mean $\tilde{S}_\alpha$ for calculating the transient response with the help of Eq. (14). Hence, the origin of the residual signal is not yet fully understood. Such signals must, however, be considered as a possible artifact in any future transient VCD experiment, in addition to pump-induced LB and LD, which can be identified more easily because of rotational diffusion. Reproducibility of a chiral signal for a number of different LO delays may be one possible test criterion, in addition to control measurements with suitable enantiomers.

## 5. Conclusions

In conclusion, we have presented an actively phase stabilized interferometer for the generation of orthogonally polarized pairs of IR femtosecond laser pulses for static and transient dichroism and birefringence measurements with multichannel detection. We were guided by the idea to combine the advantage of phase stability of a single beam measurement with the highest possible purity of polarization and its symmetry under fast modulation. By carefully orienting lenses and the sample flow-cell, we managed to maintain these conditions under the tight focusing and sample flow conditions required for time-resolved VCD experiments. We showed that the set-up is suitable for simultaneous transient linear dichroism and birefringence measurements by spectral interferometry with the same signal amplification achieved for acquiring VCD and VORD data. Pump-induced LB is expected to be the dominant background contribution in tran-

#236664 Received 20 Mar 2015; revised 27 May 2015; accepted 27 May 2015; published 12 Jun 2015

sient VCD experiments, while LB will mainly perturb transient VORD measurements. Simple rotation of the pump-beam polarization allows us to record and distinguish these signals under quasi identical experimental conditions. As a result of signal enhancement, broad band detection and referencing, transient VCD and VORD experiments with our set-up are no longer limited by signal-to-noise, which could be improved even further with already available higher laser powers and repetition rates. At wavelengths shorter than 5 $\mu$m another boost is also possible with more sensitive detector materials such as indium antimonide, as this would allow us to reduce the local oscillator intensity. However, the most important remaining difficulty for transient chiral measurements is the presence of an achiral background signal, which cannot be attributed to either transient LB or LD. We currently investigate the stability and reproducibility of this artifact, which is sensitive to beam alignment, hoping to be able to subtract it from transient data recorded for enantiomers with opposite chiral response.

## Appendix

### A. The signal field in crossed-polarizer transient linear dichroism measurements

A sample with small (pump-induced) linear dichroism $(\Delta\varepsilon_{||} - \Delta\varepsilon_{\perp})cL = \Delta\kappa L/\ln(10)$ and birefringence $\Delta\rho L = (\Delta n_{||} - \Delta n_{\perp})\pi L/\lambda$ at $\theta = 45^{\circ}$ with respect to the $x$-axis is described by the Jones Matrix

$$e^{-\frac{\kappa L}{2} - i\rho L} \begin{pmatrix} 1 - a/2 & -\frac{\Delta\kappa}{4}L - i\Delta\rho L \\ -\frac{\Delta\kappa}{4}L - i\Delta\rho L & 1 - a/2 \end{pmatrix} \tag{17}$$

where $a = (\Delta\varepsilon_{||} + \Delta\varepsilon_{\perp})/2cL\ln(10)$ is the average absorption change. The strong $x$-polarized signal-generating beam ($E_0\vec{e}_x$) gives rise to a $y$-polarized signal field

$$E_S^{achiral} = e^{-\frac{\kappa L}{4} - i\rho L}(-\Delta\kappa L/4 - i\Delta\rho L)E_0\vec{e}_y \tag{18}$$

that is transmitted by the analyzer. In full analogy to the chiral case (eqs. 10 and 11) we thus have

$$\Delta S^{\text{out of phase}} = \frac{\Delta\rho L}{\alpha} = \frac{LB[rad]}{\alpha[rad]} \tag{19}$$

$$\Delta S^{\text{in phase}} = \frac{\Delta\kappa L}{4\alpha} = \frac{LD[OD]}{\alpha[rad]}\frac{\ln(10)}{4} \tag{20}$$

### B. PEM-induced focal spot-size modulations

In the ABCD matrix description, light rays are characterized by their distance from the optical axis $r$ and the angle of inclination $\theta$, Gaussian beams by the radius of curvature $R$ of the phase front and the $1/e^2$-beam radius $w_0$. Optical elements are described by 2x2 matrices

$$M = \begin{pmatrix} A & B \\ C & D \end{pmatrix} \tag{21}$$

which act on ray vectors $v = (r, \theta)$ or change the Gaussian beam parameters according to

$$q_{out} = \frac{Aq_{in} + B}{Cq_{in} + D} \tag{22}$$

where

$$\frac{1}{q} = \frac{1}{R} - \frac{i\lambda}{\pi w_0^2} \tag{23}$$

#236664 Received 20 Mar 2015; revised 27 May 2015; accepted 27 May 2015; published 12 Jun 2015

The spatial variation of the refractive index of a square ($d \times d$) PEM is described by a cosine, which can be well approximated as quadratic function near the center:

$$\cos(\pi x/d) \approx 1 - \frac{\pi^2}{2d^2}x^2. \tag{24}$$

We can thus make use of the ABCD matrix for a Gaussian duct of length $l$, which has a quadratic radial refractive index dependence $n = n_0 \pm \frac{n_2}{2}r^2$ [35]:

$$M_{duct} = \begin{pmatrix} \cos(\gamma l) & \frac{\sin(\gamma l)}{\gamma n_0} \\ -\gamma n_0 \sin(\gamma l) & \cos(\gamma l) \end{pmatrix} \tag{25}$$

where $\gamma = \sqrt{\frac{n_2}{n_0}}$. When the PEM-induced retardation is $\pm\lambda/(2k)$ at the center of the modulator the maximum refractive index change is

$$\delta n = \frac{1}{2k}\frac{\lambda}{l}, \tag{26}$$

yielding

$$n_2 = \frac{\pi^2}{2d^2 k}\frac{\lambda}{l}. \tag{27}$$

The modulation is symmetric (contraction in $x$ direction during expansion in $y$ direction and vice versa), so we need not consider thickness variations [36]. Furthermore

$$\gamma l = \pi\sqrt{\frac{1}{2kn_0}\frac{\lambda l}{d^2}} \ll 1 \tag{28}$$

which simplifies the ABCD matrix (25):

$$M_{\text{PEM}} \approx \begin{pmatrix} 1 & \frac{l}{n_0} \\ -n_2 l & 1 \end{pmatrix} = \begin{pmatrix} 1 & \frac{l}{n_0} \\ \pm\frac{\pi^2}{2d^2 k}\lambda & 1 \end{pmatrix} \tag{29}$$

The effect of the modulator on a parallel light-ray $v = (r, 0)$ is thus the same as that of a thin lens with a focal length

$$f_{\text{PEM}} = \frac{1}{l n_2} = \pm\frac{2d^2 k}{\pi^2 \lambda} \tag{30}$$

The PEM simultaneously acts as a negative lens for light polarized in the x-direction and as a positive lens for light polarized in the y-direction and vice versa. The effect becomes stronger the longer the wavelength, but can be made smaller by increasing the size of the modulator bar. This may be the reason why this effect has not yet caused more problems in electronic CD spectrometers. In our modulator $d = 32$ mm, corresponding to a focal length of approximately 70 meters for $\pm\lambda/4$ retardation ($k = 2$) at $\lambda = 6\mu$m. We now consider two cases:

**a) Modulator in parallel beam:** For the case depicted in Fig. 6(a), PEM and lens (focal distance $f$) together act like a single lens with focal distance $f_{mod}^{-1} = f^{-1} \pm f_{PEM}^{-1}$, which is thus modulated by about $\pm 150$ $\mu$m (using $f = 100$ mm and the PEM parameters above). The beam waist near the focal spot for an initially parallel Gaussian beam ($1/R_0 = 0$, $w_0 = 4$ mm), calculated with ABCD matrix algebra, is shown in Fig. 6(c). At the average focal distance $f$ the spot size is approximately:

$$\begin{aligned} w_f^2 = \frac{\lambda}{\pi}/Im[\frac{1}{q}] &= \frac{f^2\lambda^2}{w_0^2\pi^2}\left(1 + \frac{\pi^2 w_0^4}{\lambda^2 f_{\text{PEM}}^2}\right) \\ &= w_{f_0}^2\left(1 + \frac{\pi^6 w_0^4}{4d^4 k^2}\right), \end{aligned} \tag{31}$$

#236664 Received 20 Mar 2015; revised 27 May 2015; accepted 27 May 2015; published 12 Jun 2015

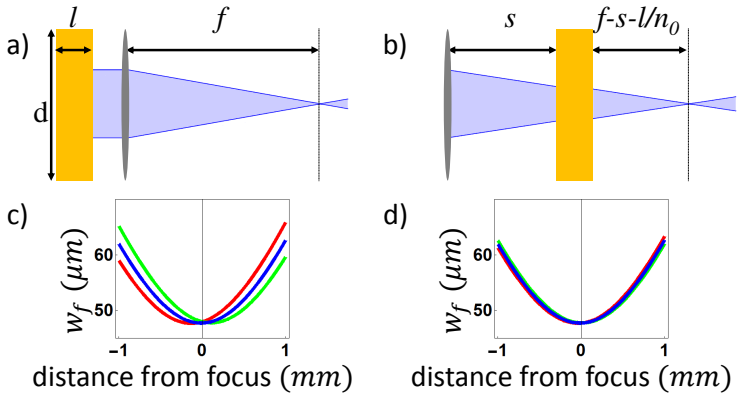


Fig. 6. (a) Beam propagation through modulator in front of lens ($f = 100$ mm). (b) Beam propagation with modulator in convergent beam 50 mm behind the lens. (c) and (d) show the corresponding Gaussian beam width $w_f \approx 0.6$ FWHM near the focus for the unmodulated beam (blue), retarded beam (red) and negatively retarded beam (green). Parameters: $w_0 = 4$ mm, $f = 100$ mm, $l = 1.5875$ mm, $\lambda = 6\mu$m, $n_0 = 2.4$, $k = 2$.

corresponding to and increase of approximately 0.5% at both $\pm\lambda/4$ retardation in our case. In practice, however, it can be difficult to place the sample exactly at the focal spot of the lens. As illustrated in Fig. 6(c), already 200$\mu$m away from the average focus the beam radius can be modulated by more than 5%.

**b) Modulator in converging beam** In CD spectrometers the PEM is often placed in between the collimating optics and the sample at the focus, as shown in Fig. 6(b). Moving the PEM close to the focus can significantly reduce the beam size modulation (Fig. 6(d)), essentially because the numerical aperture of the PEM-lensing is reduced. The optimal position for the PEM in this regard is, of course, at the focus of the collimating lens, or, in the focal plane of a telescope as in the set-up presented in this work.

In linear CD spectroscopy focal spot size modulation may cause offsets due to a different imaging of left and right handed light onto the detector. The effect is more serious when an array detector is used, because different illumination of its pixels can result in apparent spectral shifts or broadening, giving rise to large artifacts near sharp spectral features like absorption bands. This is how we first became aware of the problem in our lab. Finally, in a pump-probe experiment, a small difference in the number of excited molecules can lead to undesired time-dependent signals, which may well be of the same order as the chiral response.


## Acknowledgments

The authors thank Rolf Pfister for synthesizing the metal-spartein complexes and the authors of [31] for providing the Rhenium complex. This work was supported by the Swiss National Science Foundation (SNF) (200020_143487).


#236664 Received 20 Mar 2015; revised 27 May 2015; accepted 27 May 2015; published 12 Jun 2015